arXiv:1610.00829v1 [cond-mat.mtrl-sci] 4 Oct 2016

Polymerization of sodium-doped liquid nitrogen under pressure

M. M. E. Cormier[1,2], S. A. Bonev[2*]
[1]*Department of Physics, Dalhousie University, Halifax, Nova Scotia B3H 3J5, Canada.*
[2] *Lawrence Livermore National Laboratory, Livermore, California 94550, USA.*

(Dated: October 5, 2016)

First-principles molecular dynamics (FPMD) simulations are performed on 6 and 12% Na in dense liquid N. A detailed description of structural and electronic properties leading to an understanding of the effect of Na-doping on the polymerization phase transition of N is presented. Compression of the mixtures from 5 to 90 GPa shows three distinct regions of characteristic local order separated by pressures near 30 and 65 GPa. Computation of Gibbs free energies of mixing shows that these mixtures are thermodynamically stable beyond 20 and 15 GPa for 6 and 12 % Na respectively.

I. INTRODUCTION

High pressure (P) and temperature (T) conditions offer unique ways for the synthesis of materials with novel mechanic, optical, and electronic properties. In molecular solids and liquids, the breaking of intra-molecular bonds upon compression may lead to the formation of extended (polymeric), covalently bonded structures. The interest in such behavior is partially motivated by the potential discovery of novel energetic materials. Nitrogen, in particular, has become a subject of intense research in recent years. A polymeric structure called cubic-gauche (cg-N), which was predicted[1] among suggestions of possible stable monatomic solid phases[2,3], was eventually synthesized by Eremets *et al.*[4] at P and T above 110 GPa and 2000 K. If polymeric N is recovered to ambient P and T, it would be an energetic material with an energy capacity over five times greater than current energetic materials[4]. However, attempts to quench cg-N to ambient conditions[5–7] have been unsuccessful to date.

A possible route to metastable N is to tune the polymerization transition by combining (doping) N with small amounts of other elements. Indeed, in order to discover energetic materials with optimal properties, it is essential to explore bonding and structural properties as a function of all three fundamental variables – pressure, temperature and chemical composition. Here optimal properties include metastability at ambient conditions, polymerization transition at relatively low pressure, and high energy capacity. The last requirement suggests a focus on N-rich systems with small amounts of dopants. The fact that molecular-to-polymeric transitions are usually observed at high T also means that it is critical to understand the evolution with pressure of bonding and structural properties of molecular compounds at elevated temperatures.

Achieving these goals is challenging for a number of reasons: (i) the extreme complexity of the phase diagrams of s-p-valent materials, including numerous phases and extended regions of metastability; (ii) limitations of *in situ* measurements at high-P and T; and (iii) limitations of theoretical techniques for structure searches at high T and large crystalline unit cells (small dopant concentrations). Perhaps for these reasons, studies to day[8–12] have focused mostly on compositionally simple systems, and even their finte-T phase diagrams are not entirely known yet.

Here we have taken an alternative approach to study polymerization in N-rich systems. Investigations of liquids provide a direct way of studying the evolution of bonding properties with density at finite temperature, while avoiding many of the difficulties associated with global phase space searches of crystalline stability. The relevance of these findings for the problem of crystalline stability is grounded on the established parallels between solid and liquid structures under pressure[13–16]. The case of N is particularly favorable because of the existence of sharp and well-defined structural changes in the dense liquid[15].

In this paper, we report results on the polymerization of liquid N doped with Na. First principles molecular dynamics (FPMD) simulations are used to collect statistical information about the liquid as a function of pressure for different Na concentrations. Their structural, electronic, and thermodynamic properties are characterized, based on which distinct transition stages are identified. Our results show that only a small concentration of Na (a few %) is required to induce polymerization at sufficiently lower pressure compared to the pure N system.

II. COMPUTATIONAL METHODS

FPMD simulations of liquid N mixed with 6, 12, 25, and 50% Na, as well as pure N and pure Na, have been performed for pressures from 5 to 100 GPa along their respective 2000 K isotherms using finite-temperature density functional theory (DFT)[17] within the Perdew-Burke-Ernzerhof generalized gradient approximation (PBE-GGA)[18] as implemented in the Vienna *ab initio* simulation package (VASP) [19]. The FPMD simulations were carried out in the canonical (constant number of particles N, volume V, and temperature T) ensemble using Born-Oppenheimer dynamics and a Nosé-Hoover ther-

mostat. Supercells with periodic boundary conditions of 128 atoms were used for the Na-N mixtures and for pure liquid N, while 64 atom supercells were used for pure liquid Na. The supercells were initially randomly populated with N_2 molecules and the appropriate concentration of isolated Na atoms while enforcing a minimum separation between molecules and Na atoms. The Na concentration is measured as the ratio of the Na atoms to the total number of atoms in the system. Before compression, the liquids were confirmed to be molecular N_2 with isolated Na atoms.

To obtain well-converged pressures (within ~ 0.1 GPa) and energies ($\sim$ meV/atom), the Brillouin zone was efficiently sampled using a single $\mathbf{k}-$point at $(\frac{1}{4}, \frac{1}{4}, \frac{1}{4})$ in the Brillouin zone. Convergence tests with up to $3 \times 3 \times 3$ uniform $\mathbf{k}-$point meshes were carried out over a wide range of pressures and temperatures. Using a 0.5 fs ionic time step, each FPMD trajectory was first equilibrated within 2-3 ps and continued for additional 5 ps from which structural, electronic, and thermodynamic properties were calculated. Nine- and five-electron projector augmented wave (PAW) pseudopotentials (PP) with 2.2 and 1.6 Bohr core radii were used for all Na and N calculations respectively, using a 600 eV plane-wave cutoff energy.

For accurate determination of free energies of mixing, the PBE-GGA energies and pressures were corrected using the HSE06 hybrid functional of Heyd, Scurseria, and Ernzerhof[20]. This was done on isolated atomic configurations taken from the FPMD trajectories. The resulting corrections were averaged over the sampled snapshots. We found that five well-separated configurations from a given trajectory are sufficient to converge the average corrections for all pressures considered. The fluctuations in the energy corrections were negligible, indicating that the PBE-GGA ensemble is sufficient.

III. RESULTS

Upon compression, the Na-N mixtures exhibit three distinct regions with characteristic local structural order emerging at concentration-dependent pressures. In Section III A we describe in detail the case of 12% Na, noting that this concentration is qualitatively similar to 6 % Na, but that there are more significant differences at higher concentrations. These differences will be described in a follow-up article. The structural analysis allows for informative decomposition of the electronic properties of the liquids among characteristic clusters. The electronic properties described in Section III B clearly elucidate the effect of Na-doping on the evolution of bonding properties of N as a function of compression. Finally, thermodynamic stability as a function of concentration is analyzed for the entire pressure range considered, and concentration-dependent equations of state are presented in Section III C.

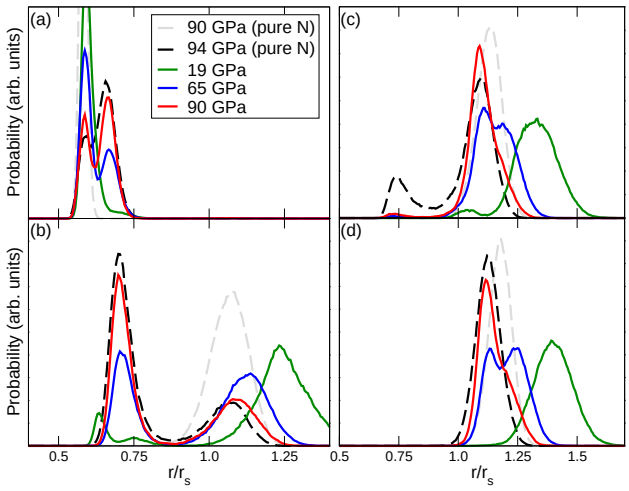

FIG. 1. Density-rescaled N-N nearest-neighbor distance distributions for the (a) 1^{st}, (b) 2^{nd}, (c) 3^{rd}, and (d) 4^{th} n.n. Results are shown for 12% Na mixture, and for pure N at several pressure as indicated in the legend.

A. Structural Properties

For the case of 12% Na, structural transitions occur near 30 and 65 GPa. These pressures mark the appearance or disappearance of some characteristic features in the local order, while compression within each region yields gradual progression of structural properties with no qualitative changes.

The initial step in the structural analysis is to calculate the distribution of nearest neighbor (n.n.) species around each atom in the supercell for every time step in the simulation trajectories. These data are used to identify distinctive atomic arrangements within the liquid – their composition, geometry, and temporal stability.

We found that the transitons are clearly marked by distinct features in the 1^{st} to 4^{th} N-N n.n. distance distributions. Fig. 1 shows a histogram of N-N neighbor distances, rescaled by the density parameter, r_s, in order to facilitate comparison between structural properties at different pressures. Here r_s is defined by $4/3\pi r_s^3 = V/N$; notice that N is the number of ions, not electrons. An appropriate cut-off radius, R_c was determined as the first minimum of the N-N pair correlation function, from which coordination fractions were determined as ensemble averages. Using this information, we define a molecule as two atoms that are mutual nearest-neighbors and both are singly-coordinated (within the cut-off radius). An n-member ring (R_n) is identified as a closed sequence of n 2-coordinated atoms . An n-member chain (C_n) is located by searching for a sequence of $(n-2)$ 2-coordinated atoms terminating on each end with atoms which are c-coordinated, where $c \neq 2$. Notice that with these definitions, if a cluster is formed by attaching a R_n to a C_m, the cluster will be identified as C_m.

First, the region below 30 GPa is characterized by a

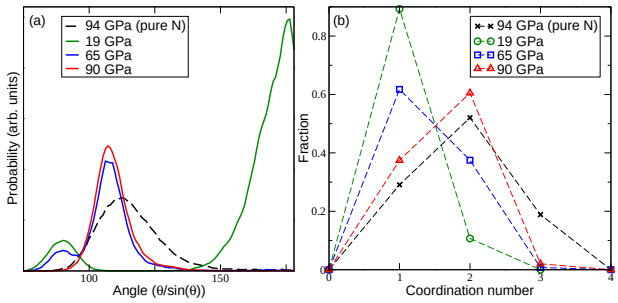

FIG. 2. (a) N-N-N angle distributions and (b) N-N coordination numbers for 12% Na concentration in liquid N. The angle distributions are calculated by taking into account only the first two n.n. within a distance less than the appropriate cut-off radius for the given pressure (see text). The N-N coordination numbers are calculated based the ensemble-averaged number of N atoms found within the cut-off radius.

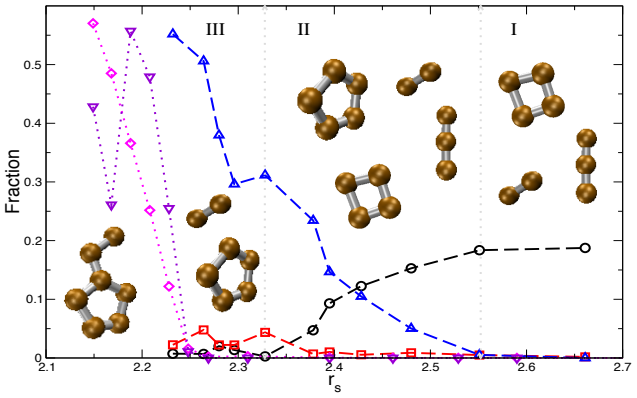

FIG. 3. The fraction of the total number of atoms in 3-member chains for 12 % Na (black-dashed circles), 4-8-member chains for 12 % Na (red-dashed squares) and pure N (magenta-dotted diamonds), and 5-member rings for 12 % Na (blue-dashed up-triangles) and pure N (violet-dotted down-triangles). The illustrations show characterisitic clusters present in each of the three regions.

broadened peak with a shoulder in the 1st n.n. distance distribution and two small peaks in the 2nd n.n. The peak in the 1st n.n. is due to N_2 molecules, the broadening comes from the first neighbor in N_3 chains (azide), and the shoulder corresponds to N_4 rings. The N_3 chains yield the first peak in the 2nd n.n. distance distribution, while the second peak is due to the formation N_4 rings. The N_2 molecules have an equilibrium bond distance very close to 1.1 Å in agreement with the chemical bond distance of isolated N_2 molecules. The N_3 chains have bond distances between 1.15 and 1.25 Å, and the N-N-N angle is nearly flat with a peak near 180 degrees (see Fig. 2) in accordance with double-bonded azide chains. The 4-member N rings are bonded with distances between 1.25 and 1.35 Å as is the case in the tetra-nitrogen molecule, corresponding to double and single bonds, and are very close to square with a peak in the N-N-N angle near 90 degrees. Thus, at pressures up to 30 GPa, even though there is a small fraction of borken N_2 molecules, the species that appear in the liquid are known from ambient-P chemistry.

Compression beyond 30 GPa causes N_3 chains to bond with N_2 molecules forming 5-member N rings. This is marked by the splitting of the 1st n.n. peak, the heightening of the first peak in the 2nd n.n., and the splitting of the peak in the 3rd and 4th n.n. The emergence of a peak at about 108 degrees in the angle distribution also marks the formation of 5-member N rings. The fraction of these rings increases with pressure while the fraction of N_3 chains decreases proportionally to the fraction of N_2 molecules (see Fig. 3 The 4-member N rings persist in this pressure region. The bond distances in the 5-member N rings are between 1.25 and 1.35 Å consistent with the lengths of double and single N-N bonds.

Further compression past 65 GPa yields N chains longer than 3 while the fraction of 5-member N rings continues to increase. The fraction of N_3 chains becomes negligible by 65 GPa as is marked by the disappearance of the first small peak in the 2nd nearest-neighbour and the disapperance of the peak at about 170 degrees in the angle distribution. The fraction of N chains longer than 3 in this region becomes non-zero and N chains of any length possess both the same N-N bond lengths between 1.25-1.35 Å, and N-N-N angle distribution has a peak at 108 degrees as the 5-member N rings. Thus, in this third region, 3-member N chains, n-member N chains, with $n > 3$, and 5-member N rings cannot be distinguished simply by observing the neighbour distributions and N-N-N angles; coordination analysis must be used to explicitely search for each cluster type. This analysis also shows that N chains in this region emerge as tails of 5-member N rings where one terminal N is 3-coordinated as a member of both a ring and a chain, with the other terminal N singly coordinated. The complete disappearance of N_4 rings does not occur until 75 GPa.

B. Electronic Density of States

The electronic density of states (EDOS) are obtained from the charge density of atomic configurations taken from the FPMD trajectories. For liquids, the ensembles are sampled and the results are averaged. In our case, we found that taking five snapshots is sufficient to obtain converged EDOS averages. For each static calculation, the Brillouin zone was sampled efficiently with 4 **k**-points at $(\frac{1}{4},\frac{1}{4},\frac{1}{4})$, $(\frac{1}{2},\frac{1}{4},\frac{1}{4})$, $(\frac{1}{2},\frac{1}{2},\frac{1}{4})$, and $(\frac{1}{2},\frac{1}{2},\frac{1}{2})$, which were given weights 1, 3, 3, and 1, respectively. This sampling approach produces better results than a uniform $3\times3\times3$ mesh, and completely reproduces results obtained with uniform $4\times4\times4$ and $6\times6\times6$ **k**-point grids. The EDOS

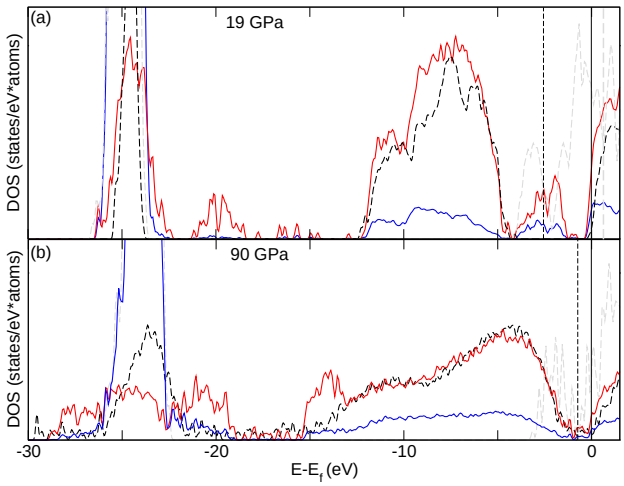

FIG. 4. Site-projected EDOS for 12% Na in liquid N showing the N (red) and Na (blue) projections along with pure N (black dashed) and pure Na (grey dashed) for (a) 19 GPa and (b) 90 GPa. The pure system DOS were shifted relative their Fermi levels to show similarities in profiles with the mixtures. The repesctive Fermi levels are shown by vertical lines for the mixtures (black-solid), pure N (black-dashed), and pure Na (grey-dashed).

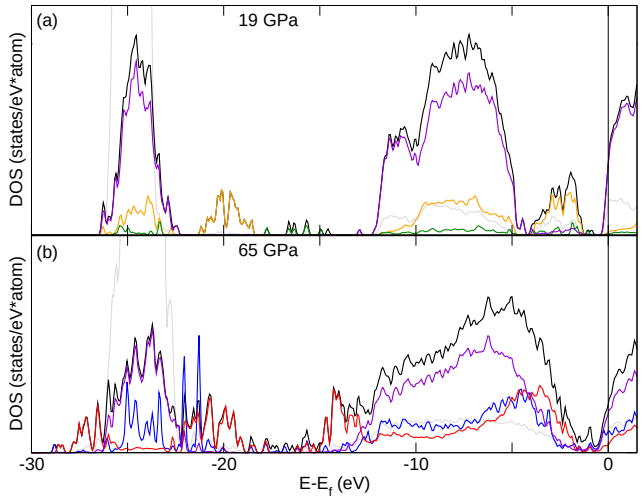

FIG. 5. Cluster decomposition of the electronic density of states for N_3 chains (orange), N_2 molecules (violet), N_4 rings (green), 5-member N-rings (red), and n-member N-chains, $n \geq 3$ (blue). The total projections are also shown for N (black) and Na (grey).

are projected on the N and Na species (Fig. 4) and further decomposed based on the types of clusters that the atoms are part of (Fig. 5). Site-projections were obtained by choosing a cut-off radius of half the 1st coordination shell radius. As a consequence, small overlaps were incurred, but features from higher energy states that were otherwise missed became apparent.

At 19 GPa (region I of the mixed system) pure N is still an insulator with a band gap of about 5 eV. The Na atoms contribute electronic states in this band gap region. As a result, there is a small amount of occupied states at the Femi level of the Na-doped system - partial occupancy of the anti-bonding orbitals of the N_2 molecules. Furthermore, additional EDOS appear below the Fermi level, which belong mostly to N_3 chains. These are formed with extra electronic charge transferred from the Na atoms. Meanwhile, the valence states due to N_2 molecules remain very similar to those in pure liquid N. The molecular states around -30 eV are broadened compared to the pure case and the appearance of states around -20 eV are strictly due to N_3 chains.

With increasing density, the edge of the molecular states is broadened towards the Fermi level until it overlaps with the N_3 states in the gap. At this point, around 30 GPa, the formation of 5-member N rings, by combining N_2 molecules with N_3 chains, is possible. As more rings form, the states within the gap are completely overtaken. Notice that states owing to $n-$member chains ($n \geq 3$) are nearly identical to 5-member rings, except for the lower energy stabilizing states around -14 eV.

Compression beyond 65 GPa into region III yields no qualitative changes in the electronic structure. The fraction of N_2 molecules decreases and so the total number of states due to various clusters changes, but there is no qualitative change in profile of the EDOS.

We see that the mechanism of polymerization here is different than in pure N where the molecules remain stable until the electronic band gap closes at around 90 GPa and the liquid becomes metallic. Small amounts of Na are sufficient to change significantly the electronic structure of the liquid by facilitating the formation of N_3 clusters with states below the Fermi level. The latter become precursors for the breaking of the already weakened N_2 molecules and the formation of poly-N at pressure much lower than 90 GPa.

C. Free Energy of Mixing and Equation of State

Here we examine the thermodynamic stability of the liquids by computing their Gibbs free energies. Pressures, temperatures and energies were calculated from ensemble (time) averages, while entropies were determined following the method outlined in Ref. 21. We then calculate the Gibbs free energies of mixing of the liquids as $\Delta G_{mix} = G_{(N-Na)_i} - x_i G_N - (1-x_i) G_{Na}$, where x_i is the concentration of N in mixture $(N-Na)_i$ and each G_X term on the right hand side is the Gibbs free energy per atom of liquid X.

The results in Fig. 6 show that the mixtures are thermodynamically stable with respect to the pure systems beyond a maximum of ~ 23 GPa. Hybrid functional corrections are shown to be largest in the transition region, but yield corrections in favor of the mixtures.

The equations of state for pure liquid N, N mixed with 6, and 12 % Na, and pure liquid Na are shown in Fig. 7

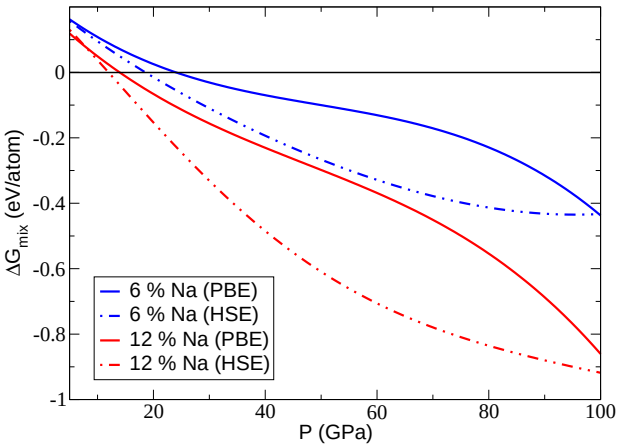

FIG. 6. Gibbs free energies of mixing as a function of pressure with (dotted-dashed) and without (solid) HSE corrections for 6 and 12 % Na in liquid N.

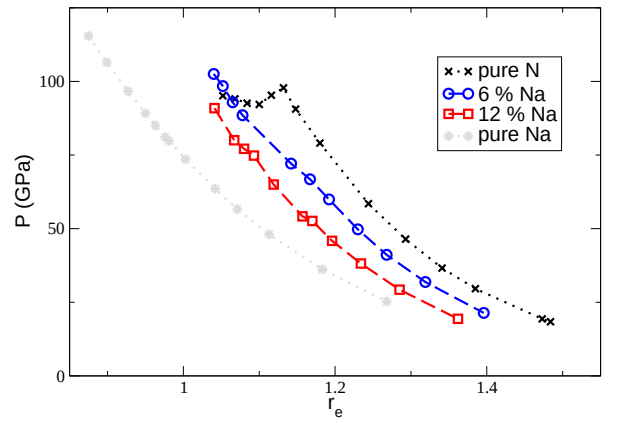

FIG. 7. Equations of state. The pressure is plotted against the valence electron density, r_e (see text for details).

The pressure is plotted against the valence electron density parameter, r_e, defined as $V_e/N_e = (4/3)\pi(r_e a_0)^3$. Here $V_e = V - V_{ion\ core}$, where $V_{ion\ core}$ is the volume assigned to electron cores. It is calculated by taking the core radius as the Wigner-Seitz radius from the pseudopotentials. N_e is the number of valence electrons implemented in the pseudopotentials, and a_0 is the Bohr radius. At the same pressure, the valence electron density increases with Na-doping concentration. Thus, the Na subsystem chemically compresses the N subsystem, catalyzing the formation of 5-member N rings and n-member chains, $n \geq 3$.

IV. CONCLUSION

We have characterized the structural, electronic, and thermodynamic properties of Na-doped liquid N as a function of pressure. The polymerization transition develops in three stages and commences at much lower pressures compared the the pure N system even with small Na concentrations. We have elucidated the mechanism by which Na promotes this transition.

In the case of pure liquid N, the valence states are broadened upon compression, where at the transition pressure the system metallizes, destabilizing N_2 molecules. At low pressure, the presence of Na destabilizes N_2 bonds by donating its valence electron, yielding the preferred N_3 azide chains. Assisted by the chemical compression owing to Na ions, the valence states of N_2 molecules are broadened upon compression, overlapping with the mid-gap states of the N_3 chains, yielding the preferred N_5 rings. Further compression continues to break N_2 molecules. The role of Na is then two-fold: to provide additional electrons that destabilize molecular bonds, and to chemically compress the N subsystem, yielding a 2nd-order phase transition that does not fully metallize at high P. This is in contrast to the first-order liquid-liquid phase transition of pure liquid N induced by metallization.

V. ACKNOWLEDGMENTS

Work performed under the auspices of the US Department of Energy under contract No. DE-AC52-07NA27344. Computational resources were provided by Acenet and Livermore Computing.

* Electronic address:bonev@llnl.gov

[1] C. Mailhiot, L. H. Yang, and A. K. McMahan, Phys. Rev. B **46**, 14419 (1992).
[2] A. K. McMahan and R. LeSar, Phys. Rev. Lett. **54**, 1929 (1985).
[3] R. M. Martin and R. J. Needs, Phys. Rev. B **34**, 5082 (1986).
[4] M. I. Eremets, A. G. Gavriliuk, I. A. Trojan, D. A. Dzivenko, and R. Boehler, Nature Materials **3**, 558 (2004).
[5] T. W. Barbee III, Phys. Rev. B **48**, 9327 (1993).
[6] T. Zhang *et al.*, Phys. Rev. B **73**, 094105 (2006).
[7] X.-Q. Chen, C. L. Fu, and R. Podloucky, Phys. Rev. B **77**, 064103 (2008).
[8] B. A. Steele and I. I. Oleynik, Chemical Physics Letters **643**, 21 (2016).
[9] B. A. Steele and I. I. Oleynik, Journal of Chemical Physics **143**, 234705 (2015).
[10] X. W. et *al.*, Journal of Chemical Physics **141**, 044717 (2014).

[11] X. W. et *al.*, Journal of Chemical Physics **139**, 164710 (2013).
[12] M. I. E. et *al.*, Journal of Chemical Physics **120**, 10618 (2004).
[13] I. Tamblyn, J.-Y. Raty, and S. A. Bonev, Physical Review Letters **101**, 075703 (2008).
[14] I. Tamblyn and S. A. Bonev, Physical Review Letters **104** (2010).
[15] B. Boates and S. A. Bonev, Phys. Rev. Lett. **102**, 015701 (2009).
[16] B. Boates and S. Bonev, Phys. Rev. B **83**, 174114 (2011).
[17] W. Kohn and L. Sham, Phys. Rev. **140**, A1133 (1965).
[18] J. Perdew, K. Burke, and M. Ernzerhof, Phys. Rev. Lett. **77**, 3865 (1996).
[19] G. Kresse and J. Hafner, Phys. Rev. B **47**, 558 (1993); Comp. Mat. Sci. **6**, 15 (1996).
[20] J. Heyd, G. Scuseria, and M. Ernzerhof, J. Chem. Phys. **121**, 2780 (2003).
[21] A. M. Teweldeberhan and S. A. Bonev, Physical Review B **83**, 134120 (2011).